Classification: Biological & Physical Sciences, Environmental Sciences

Divergent responses of Atlantic coastal and oceanic *Synechococcus* to iron limitation

Katherine RM Mackey[1,2,*], Anton F Post[2], Matthew R McIlvin[1],

Gregory A Cutter[3], Seth John[4], and Mak A Saito[1,*]

[1]Marine Chemistry and Geochemistry, Woods Hole Oceanographic Institution, Woods Hole MA 02536

[2]Bay Paul Center for Comparative Molecular Biology and Evolution, Marine Biological Laboratory, Woods Hole, MA 02543

[3]Ocean, Earth, and Atmospheric Sciences, Old Dominion University, Norfolk, VA 23529

[4]Department of Earth and Ocean Sciences, University of South Carolina, Columbia, SC 29208

* corresponding authors, kmackey@uci.edu, 301.356.4041 and msaito@whoi.edu, 508.289.2393

Abstract

Marine *Synechococcus* are some of the most diverse and ubiquitous phytoplankton, and iron (Fe) is an essential micronutrient that limits productivity in many parts of the ocean. To investigate how coastal and oceanic Atlantic *Synechococcus* strains acclimate to Fe availability, we compared the growth, photophysiology, and quantitative proteomics of two *Synechococcus* strains from different Fe regimes. *Synechococcus* strain WH8102, from a region in the southern Sargasso Sea that receives substantial dust deposition, showed impaired growth and photophysiology as Fe declined, yet utilized few acclimation responses. Coastal WH8020, from the dynamic, seasonally variable New England shelf, displayed a multi-tiered, hierarchical cascade of acclimation responses with different Fe thresholds. The multi-tiered response included changes in Fe acquisition, storage, and photosynthetic proteins, substitution of flavodoxin for ferredoxin, and modified photophysiology, all while maintaining remarkably stable growth rates over a range of Fe concentrations. Modulation of two distinct ferric uptake regulator (Fur) proteins that coincided with the multi-tiered proteome response was found, implying the coastal strain has different regulatory threshold responses to low Fe availability. Low nitrogen (N) and phosphorus (P) availability in the open ocean may favor the loss of Fe response genes when Fe availability is consistent over time, whereas these genes are retained in dynamic environments where Fe availability fluctuates and N and P are more abundant.

Key words: iron adaptation, *Synechococcus*, photosynthesis, quantitative proteomics

Significance Statement

Conventional knowledge suggests that coastal phytoplankton are less able to adapt to Fe limitation than open ocean species. Here we show that in contrast to the established paradigm, coastal *Synechococcus* from the New England Shelf is capable of dynamic, multi-tiered Fe adaptation that allows it to thrive over a broad range of Fe concentrations by partitioning Fe among different uptake and storage proteins. This protein-based response is beneficial in high nitrogen (N) waters with low and variable Fe:N ratios. Oceanic *Synechococcus* lacks this adaptive response, suggesting the small yet significant N cost of retaining Fe response proteins offsets the benefit of Fe adaptability in the southern Sargasso Sea, where N is chronically scarce and Fe:N ratios are high.

\body

The marine *Synechococcus* are a cosmopolitan group of cyanobacteria that contribute approximately 17% of marine net primary production worldwide[1], and whose diversity is linked to nutrient availability in both coastal and open ocean waters[2]. Of the nutrients required by phytoplankton, the micronutrient iron (Fe) limits productivity in ~30% of the world's oceans[3] and shapes *Synechococcus* genome content[4,5]. Seawater Fe concentrations in the euphotic zone can vary due to inputs from atmospheric, coastal, and upwelled sources. The open ocean, being more removed from these sources, is typically depleted in Fe relative to coastal waters. Consistent with these distributions, experiments on oceanic phytoplankton have found them able to grow at lower metal conditions than related coastal strains, implying a general phenomenon of open ocean phytoplankton being better adapted to low metal availability[6,7].

The North Atlantic Ocean presents an extreme endmember with which to examine the coastal-open ocean phytoplankton adaptation phenomenon due its large Fe flux associated with seasonal atmospheric dust deposition from the Saharan desert[8,9]. Moreover, there has been increasing evidence that Fe availability may be dynamic in coastal regions, with observations of Fe limitation of phytoplankton in eastern boundary upwelling regions upon upwelling of macronutrient-rich and Fe-depleted waters[10,11]. While the diversity and distribution of *Synechococcus* strains have been linked to macronutrient availability[2], the considerable range of Fe levels across which *Synechococcus* thrive suggests they may also possess unique and diverse regulatory mechanisms for Fe acclimation.

To explore this acclimation potential in the North Atlantic context, we compared the responses of coastal and oceanic Atlantic *Synechococcus* to Fe limitation. Comparison of strain

origins with recent trace metal and low-level nutrient measurements from the recent US North Atlantic Zonal Transect GEOTRACES expedition demonstrates large differences in nitrate, phosphate and dissolved Fe between sites in the North Atlantic basin. The coastal strain, WH8020, was isolated from the New England Shelf (Fig. 1A,B), a region with a dynamic nutrient[12] and Fe[13] regime. Oceanic strain WH8102 was isolated from the permanently stratified southern Sargasso Sea, an oligotrophic site that consistently receives Fe from aeolian dust year round, with very high levels in the summer[8]. The consistent dust supply results in higher dissolved Fe levels in the open ocean (~0.8nM within the Sahara dust plume) relative to North American coastal waters (Fig. 1B).

To test their abilities to acclimate, both strains were rendered Fe-limited by sequential transfer into no-Fe-added media and were rescued with varying concentrations of Fe' (Fe' defined as the sum of inorganic species). Cellular protein was harvested during log-phase growth to characterize Fe responses (Fig. 2C,H). Protein abundance was measured following cell pellet extractions of single cultures grown at each prescribed Fe concentration, followed by high-resolution LC-MS proteomic analysis for relative abundance and targeted proteomics for absolute abundance (methods in SI).

We observed that the growth rate and photophysiology (F_v/F_M) of oceanic *Synechococcus* WH8102 was proportional to Fe' concentration (Fig. 2A-D). In contrast, coastal *Synechococcus* WH8020 tailored its response to Fe limitation through the differential expression of Fe response proteins in a multi-tiered, hierarchical cascade by which cells partitioned and conserved Fe, and so thrived over a broad range of Fe concentrations. Fe' levels had a minimal effect on growth rate (Fig. 2F), although a sharp decline in photosynthetic protein abundance was observed below 1 nM (Fig. 2J), followed by a decline in photosynthetic efficiency below 0.3 nM (Fig. 2I).

Thresholds for photosynthetic efficiency and photosynthetic protein abundance were similar between strains (Fig. 2D,E,I,J).

The global proteome of coastal *Synechococcus* WH8020 revealed large changes in the abundance of Fe sensing, acquisition, and storage proteins (Fig. 3A). Fe' levels ≤1 nM led to induction of the Fe transport protein, IdiA, that assists in Fe uptake during periods of low Fe availability[14], and substitution of Fe-free flavodoxin for Fe-requiring ferredoxin[15,16]. At Fe' levels above 1 nM, coastal WH8020 produced ferritin, which stores Fe when it is abundant for later use when levels decline. Several additional Fe response systems were present in WH8020 that are also shared in the genome of coastal strain CC9311 isolated from the California Coastal Current, although the latter has additional genes including a ferrous Fe uptake protein (*feo;* Fig. 3B; SI Appendix Table S1). The strong proteome response of coastal WH8020 to low Fe implies that coastal Atlantic waters may share aspects of the "patchwork mosaic" dynamics of Fe limitation and excess similar to California coastal waters[10,11].

The multi-tiered response in coastal WH8020 appears to be regulated by two isoforms of the ferric uptake regulator protein (Fur), which acts as a transcriptional repressor when it binds intracellular Fe(II)[17]. Interestingly, the two Fur isoforms quantified here appeared to respond to different Fe' concentrations, and may govern "Fe limited" and "Fe stressed" conditions respectively (Fig. 3A).

In contrast to the coastal strain, oceanic WH8102 did not show a multi-tiered proteome response to Fe limitation and lacked many of the Fe response genes discussed above. Oceanic WH8102 lacks flavodoxin, although at least one of its ferredoxin proteins was still regulated by Fe' levels (Fig. S1). Both WH8102 and WH8020 genomes have more than one ferredoxin

115 isoform that may have different physiological or regulatory roles (SI Appendix, Table S1).
116 Additionally, the coastal WH8020 genome contains both ferritin (1188) and heme-based
117 bacterioferritin (2623)[18,19], while oceanic WH8102 lacks both based on sequence homology.

118 This study belies the expectation that oceanic phytoplankton would tend to experience
119 greater Fe stress than coastal phytoplankton[6] for two reasons. First, certain open ocean regions
120 like the southern Sargasso Sea can have relatively high and stable dissolved Fe levels depending
121 on their location (Fig. 1B). Second, as we show here, the underlying factor governing Fe
122 acclimation capacity is not Fe availability alone, but the simultaneous pressure exerted by
123 multiple scarce nutrients, in particular N, P, and Fe. The Fe-adaptations of coastal WH8020
124 (relative to WH8102) require P for genome maintenance and N for protein synthesis. These costs
125 can be estimated by examining genomic content and by using quantitative proteomic
126 measurements. Overall, oceanic WH8102 has a ~10% smaller genome than either coastal strain
127 (WH8020 and CC9311), consistent with the loss of Fe response genes like those encoding
128 ferritin and flavodoxin (Fig. 3B, SI Appendix Table S1). This smaller genome likely imparts a
129 selective advantage during P-limited periods in the south Sargasso Sea[20,21]. Yet the cost of
130 maintaining a single Fe-adaptive gene within the Synechococcus WH8102 genome is only
131 ~0.04% of the genome P content (1 gene in 2526 genes total), implying that maintaining each
132 individual gene would incur only a small ecological cost.

133 The N cost associated with the multi-tiered Fe-adaptive response in coastal WH8020 was
134 examined using quantitative proteomic methods, where isotopically-labeled peptide internal
135 standards were synthesized for ferritin, IdiA, ferredoxin, and flavodoxin, and quantified using
136 multiple reaction monitoring on a quadrupole-orbitrap mass spectrometer[22]. N requirements were
137 calculated based on the absolute concentration and chemical formula of each protein (see

Methods). Ferritin and IdiA synthesis requires approximately 3.3-4.4 pmol N per μg of total protein (Fig. 3C). Because the cells must either synthesize ferritin or IdiA depending on ambient Fe concentrations, these Fe-adaptive proteins incur an N cost for the cell regardless of whether Fe levels are high (for Fe storage) or low (for Fe uptake). Flavodoxin has the largest N cost (14.7 pmol N/μg total protein; Fig. 3C) of the Fe-adaptive proteins targeted here. The ~100 fold greater abundance of flavodoxin (98.9 fmol per μg total protein) compared to ferredoxin (0.73 fmol per μg total protein) in WH8020 is consistent with reports of flavodoxin's lower reaction efficiency compared to ferredoxin[23]. While flavodoxin only contributes to ~0.2% of total protein N at its most abundant (0.0019 μg flavodoxin per μg total protein), this observation suggests that even the small N costs associated with adaptive responses to nutrient scarcity are ecologically significant, and this is consistent with previous findings on the adaptive responses to vitamin B_{12} scarcity in diatoms[24]. The benefit that flavodoxin imparts in the dynamic coastal ocean likely outweighs the N cost of its synthesis. Moreover, the small N cost of synthesizing Fe-response proteins like flavodoxin is still higher than the P cost of maintaining the corresponding genes.

Our results suggest that the capacity of *Synechococcus* to adapt to Fe-limitation therefore depends not on Fe alone, but on the balance between availability of Fe, N, and P. The combination of relatively high dissolved Fe levels[25] and scarcity of N and P in the permanently stratified southern Sargasso Sea may place stronger selective pressure on oceanic WH8102 to eliminate Fe-adaptive genes. A recent North Atlantic transect that sampled near both *Synechococcus* isolation environments illustrates this: oceanic surface waters had elevated Fe:nitrate ratios (11.4:1), while the Atlantic coast had relatively lower Fe:nitrate (5.3:1; Fig. 1C). Additionally, mid-ocean seawater nitrate:phosphate ratios were low (~2.1:1) relative to both the Redfield ratio[26] (16:1) and WH8102 cell quotas (10.9:1 and 43.8:1 in P-replete and P-limited

cultures respectively[27]). These nutrient availability patterns are consistent with a selection pressure against expending additional N within Fe-adaptive proteins in the oligotrophic southern Sargasso Sea. Specifically, low N levels in the open ocean may make flavodoxin less beneficial for oceanic WH8102, given that less Fe adaptability would be needed under its relatively stable Fe regime (Fig. 1B,C). Oceanic WH8102 is likely well-suited to these high dust waters, whereas other oceanic strains with greater Fe acclimation capacity may exist in regions with lower Fe availability, such as the Equatorial Pacific[28] and Costa Rica Dome[29], or even seasonally in the northern Sargasso Sea near the Bermuda Atlantic Time Series (BATS; Fig. 1A) where dust supply wanes seasonally[9] and Fe is depleted within the deep chlorophyll maximum[30].

In comparison to *Synechococcus*, the N cost of Fe adaptability is apparently not sufficient to deter the highly streamlined *Prochlorococcus* MED4 and MIT9301 genomes from retaining flavodoxin, yet ecotypes adapted to chronic Fe limitation in the Pacific Ocean have eliminated certain Fe-containing genes from their genomes[28]. The selective loss of Fe-containing proteins (but not Fe-free Fe response proteins like flavodoxin) from *Prochlorococcus* genomes implies a particular importance of adapting to Fe scarcity in *Prochlorococcus*. *Prochlorococcus* has approximately two-fold lower cellular N requirements than *Synechococcus*[27], and obtains N from urea[31,32]. As a result, *Synechococcus* may experience greater selective pressure to conserve N given that smaller *Prochlorococcus*, with its larger surface area to volume ratio, would likely outcompete *Synechococcus* for Fe in either case.

These results demonstrate distinct responses of marine *Synechococcus* from coastal and open Atlantic Ocean environments. The surprising dynamic, multi-tiered Fe response of coastal *Synechococcus* WH8020 implies that periods of Fe scarcity likely extend well into the coastal zones of continental shelf regions, in addition to the open ocean and coastal upwelling systems.

The limited response of oceanic *Synechococcus* WH8102 demonstrates the challenge of multi-nutrient scarcity in the open ocean, where the advantages of maintaining Fe-adaptability are offset by even small nutritional costs. These responses suggest that the need to conserve Fe plays an important role in species evolution in the coastal and open ocean, but the outcome rests on a complex interplay between the availability of multiple scarce nutrients and an organism's complement of biochemical responses.

Materials and Methods

Strains and culturing conditions. *Synechococcus* sp. strain WH8102 was isolated from surface waters in the oligotrophic southern Sargasso Sea (22.495°N, 65.6°W by F. Valois and J. Waterbury) north of Puerto Rico where the waters are permanently stratified, and belongs to *Synechococcus* clade III[2]. Strain WH8020 was isolated from surface waters near Woods Hole MA (38.68°N, 69.32°W by F. Valois and J. Waterbury). Both strains were generously provided by the Waterbury lab. The WH8102 genome is available at http://www.ncbi.nlm.nih.gov/Taxonomy/Browser/wwwtax.cgi?id=84588. The WH8020 genome has been submitted to NCBI and has the following submission identifiers: Submission ID: SUB871617; BioProject ID: PRJNA278997; BioSample ID:SAMN03436066; Organism: Synechococcus sp. WH 8020.

Synechococcus spp. WH8102 and WH8020 were cultured at 23^{o}C under 10 μmol quanta m^{-2} s^{-1} constant white light provided by a mixture of fluorescent cool white and grow light bulbs. Microwave sterilized media was based on a modified SN media recipe for trace metal cultivation, and consisted of oligotrophic seawater diluted 25% with MilliQ water and amended with nutrients and trace metals: 2 mM $NaNO_3$, 0.2 mM NH_4Cl, 140 μM K_2HPO_4, 100 μM Na_2CO_3, 10 μM ethylenediaminetetraacetic acid disodium salt (EDTA), 1.42 μM $MnCl_2$.4H2O, 0.32 μM$Na_2MoO_4.2H_2O$, 0.15 μM $ZnSO_4.7H_2O$, 0.17 μM $Co(NO_3)_2.6H_2O$, and 6.5 μM citric acid. The seawater was collected on the CoFeMUG Cruise in 2007 from the mid-Atlantic Ocean and had a total Fe concentration of 0.1 nM at the time of collection[33]. Given the 10 μM EDTA added to the media, this background contributed 0.004 nM Fe' to the overall Fe' content. Additional Fe was added back to the seawater as $FeCl_3$ at various concentrations described below.

To induce iron limitation, cells were transferred successively into fresh no-Fe-added media that contained all other media components until growth limitation was observed. FIRe fluorescence was monitored to determine when stationary phase was reached based on raw fluorescence growth curves and F_v/F_M values (see FIRe methods below). Cells were maintained under these Fe-limited stationary conditions for at least 2 weeks. The Fe-limited parent culture was then used to inoculate 8 new single-replicate flasks containing 200 mL of fresh medium. The Fe concentrations added to these flasks were 2533, 253, 25, 13, 7, 3, 0.7, and 0 nM added total $FeCl_3$ from a single stock prepared fresh in weakly acidified MilliQ water, and all culture flasks had 10 μM EDTA regardless of the concentration of Fe added. Iron concentrations were measured using a coastal seawater method[34] on an inductively coupled plasma mass spectrometer for the two most concentrated batches of media. The coefficients of variation were <7% for these measurements. The values (2645±198 nM and 2420±14 nM) were averaged (2533 nM), and dilutions were calculated based on that number to arrive at the numbers above for each treatment, which includes the background concentration in the seawater (0.1 nM total Fe).

The sum of inorganic iron species (Fe') was estimated using a factor of Fe'/Fe_{Total} = of 0.039, based on empirical determination of the FeEDTA dissociation constant and resultant Fe' in seawater media with an equivalent 10 μM EDTA in darkness at 20°C[35]. This yielded free Fe' concentrations of 100, 10, 1, 0.5, 0.3, 0.1, and 0.03 nM respectively. Constants and values for Fe' in light were also available (Fe'/Fe_{Total} = 0.065), but because the illumination used was much stronger than that of this experiment (10 versus 500 μmol quanta m^{-2} s^{-1}), the dark results seem more representative of our experimental system. The background Fe' concentration in the seawater was 0.004 nM. The Fe' value is the amount considered to be accessible to iron transport systems, while organically chelated iron (FeEDTA or natural iron ligands[36]) may be accessible

through reductase or siderophore transport systems. No organic chelated iron acquisition systems are currently known in marine *Synechococcus*.

FIRe fluorescence (F_v/F_M, see below) was monitored daily. Cultures for protein analysis were harvested during late log phase by gentle vacuum filtration onto 0.2 μm Supor filters and frozen at -80^{o}C until processing.

Protein extraction and digestion. Frozen cell samples for protein extraction were rinsed from the filters in 100 mM ammonium bicarbonate, sonicated on ice a minimum of 10 min to lyse cells and break up membranes, and centrifuged to pellet cell debris. Proteins in the supernatant were precipitated overnight in 100% acetone at -20^{o}C. The pellet was resuspended in 6 M urea with 0.1 mM ammonium bicarbonate, reduced with 10 mM dithiothreitol (56^{o}C, 450 rpm, 1 hr), and alkylated with 30 mM iodoacetamide (20^{o}C on bench for 1 hr). Proteins were then digested with trypsin (Promega Trypsin Gold; 37^{o}C, 400 rpm overnight) at an enzyme : protein ratio of 1:50. The tryptic peptides were concentrated by evaporation and resuspended in 2% acetonitrile with 0.2% formic acid.

Global proteome analysis. Chromatography and tandem mass spectrometry (LC-MS/MS) of the tryptic peptides was performed on a Q Exactive (QE) Orbitrap mass spectrometer (Thermo Scientific). Chromatography was performed using a 180 minute nonlinear gradient of 0.1% formic acid in water and 0.1% formic acid in acetonitrile on a 25 cm x 100 μm column (New Objective PicoTip emitter PicoFrit) packed with 3 μm C18 silica packing material (Reprosil-Gold 120 C18, 3 μm, Dr. Maisch GmbH). Tandem mass spectrometry was performed on the top 15 ions. Full MS scans were performed at 70k resolution with a scan range of 380 to 2000 m/z

and 1e6 AGC target. Data dependent MS2 scans were monitored at 17.5k resolution with 1e5 AGC target, 100 ms maximum injection time, and a 2.0 m/z isolation window.

Proteins were identified against the genome for each strain using the SEQUEST algorithm within Proteome Discoverer (Thermo) and normalized spectral counts tabulated in Scaffold software (Version 4.3.2 Proteome Software Inc.). Protein identification criteria included a protein identification probability of 99%, a peptide identification probability of 95%, and identification of two or more peptides from the protein's sequence using the Peptide Prophet algorithm[37]. Relative protein abundance data was normalized to total spectral counts. The global data was then imported into Cluster 3.0[38], log transformed, centered on mean, and normalized across treatments to create a heatmap (Fig. 2). Proteins were clustered using the correlation (uncentered) similarity metric and centroid linkage options.

The global proteome values show the spectral counts for each protein, which are uncalibrated measurements of relative abundance for which comparisons within a protein across treatments is the best application. In contrast, the targeted calibrated measurements for which isotopically labeled peptide standards are used (see below), are the appropriate measurement for comparisons of concentrations of different proteins.

Targeted protein quantitation. Peptide target sequences representing proteins of interest were identified from peptides in the global proteome. Two peptides per protein of interest were synthesized using SpikeTides Synthetic Proteotypic Peptides (JPT Peptide Technologies GmbH). These peptide standards are labeled with trypsin-cleavable stable isotope markers ("heavy" peptides), allowing precise quantitation of the peptide. Experimental samples were spiked with known amounts of each standard in order to determine the amount of the respective protein in the

sample on a fmol peptide/ μg total protein basis. Samples were analyzed using parallel reaction monitoring (PRM, see SI Appendix Table S4 for settings)[39,40], where each precursor ion (light and heavy masses) was selected by the quadrupole, fragmented, then all fragment ions were quantified in the orbitrap[22]. The sum of the top five fragment ion intensities was calculated in Skyline (MacCoss Lab Software version 3.1) and used to estimate peptide signal intensity. Peptide concentration was calculated based on the ratio to the heavy peptide standards that were added in known quantity.

To compare the amount of protein under Fe replete and deplete conditions, all PRM values above (replete) and below (deplete) the Fe threshold for that protein were averaged and compared for both peptides per targeted protein (Table S2). For example, for flavodoxin the threshold for WH8020 occurred for cells grown between 1 and 10 nM, so all protein concentrations for cells grown at ≥10 nM were averaged to obtain the replete, or "high", protein concentration, and all values for cells grown at ≤1 nM were averaged to obtain the deplete, or "low", protein concentration. The replete and deplete values were subtracted to determine the mass of extra protein produced by the cell when these genes are expressed. The N cost associated with each protein was calculated based on the number of N atoms per protein for each target.

Fe response gene identification. The WH8102 and CC9311 genome annotations were searched using iron-related key words. The identified genes were used to BLAST the WH8020 genome to identify orthologous genes.

Photosystem II fluorescence. Photosystem II fluorescence was measured using a FIRe fluorometer with FIReview software (Satlantic) and blue excitation light (450 nm with 30 nm bandwidth). Due to the small cross section of *Synechococcus* for blue light, it is necessary to

increase the duration of the saturating flash beyond the default value to ensure that a steady state fluorescence plateau is reached; in this study a single turnover flash duration of 200 μs was used. Default values were used for all other parameters. The reference excitation profile was recorded for these timing parameters using rose bengal dye. The fluorescence parameters F_v/F_M (photosynthetic efficiency in the dark-adapted state) was determined using the curve fitting program in FIRePro with the relaxation kinetics fitting disabled. The F_v/F_M of each culture was monitored daily following re-addition of Fe to the WH8102 and WH8020 cultures.

Growth Curves. Doubling times in figure 2A,F were calculated from fluorescence growth curves shown in figure 2C,H using the equation $T_d = [(t_f-t_i)\ln 2]/[\ln(c_f/c_i)]$, where T_d is the time for the population to double, t_f is final time, t_i is initial time, c_f is the final concentration, and c_i is the initial concentration. Fluorescence trends were confirmed against flow cytometry measurements of samples taken on the final time point of each experiment (Figure S2). Formalin fixed samples were flash frozen in liquid nitrogen and stored frozen at -80^{o}C until analysis on an Accuri flow cytometer. Counts were triggered on chlorophyll fluorescence. These data are shown in SI Appendix Figure S2, and R^2=0.94.

Threshold response calculations

For Fig.2, protein thresholds were determined as the concentration at which the protein declined to 50% of its maximal value. Photophysiological thresholds were taken as the concentration above which the F_v/F_M response diverged from the "no iron added" condition".

Nutrient and dissolved Fe concentrations.

Seawater samples for Fe concentration analysis were collected on US GEOTRACES section GA03 using trace-metal clean sampling protocols[41]. Fe concentrations were analyzed on a

Neptune multi-collector ICP-MS at the University of South Carolina by isotope dilution, after concentrating and purifying Fe from a 1 L seawater samples[42,43]. Nanomolar concentrations of dissolved phosphate, nitrate, and nitrite were determined on board ship using conventional automated nutrient analyzer methods modified for the use of 250 cm long liquid core waveguides as described previously[44,45].

Acknowledgements

This work was supported by a National Science Foundation Postdoctoral Research Fellowship in Biology to K.R.M.M. (NSF 1103575), National Science Foundation Oceanography grants OCE-1220484, OCE-0928414, OCE-1233261, OCE-1155566, OCE-1131387, and OCE-0926092, as well as Gordon and Betty Moore Foundation grants 3782 and 3934. We are grateful to John Waterbury and Frederica Valois for helpful discussions and culture strains, and Madeli Castruita for discussion on bacterioferritin sequences.

Author contributions

KRMM, MAS, and AFP conceived and designed the experiments, KRMM and MRM conducted the experiments and analysis, AFP, SJ and GAC contributed data, KRMM and MAS wrote the paper, and all authors provided comments on the paper.

References

1. Flombaum, P. *et al.* Present and future global distributions of the marine Cyanobacteria Prochlorococcus and Synechococcus. *Proc. Natl. Acad. Sci.* **110,** 9824–9829 (2013).
2. Scanlan, D. J. *et al.* Ecological Genomics of Marine Picocyanobacteria. *Microbiol. Mol. Biol. Rev.* **73,** 249–299 (2009).
3. Moore, C. M. *et al.* Processes and patterns of oceanic nutrient limitation. *Nat. Geosci.* **6,** 701–710 (2013).
4. Palenik, B. *et al.* The genome of a motile marine Synechococcus. *Nature* **424,** 1037–1042 (2003).
5. Palenik, B. *et al.* Genome sequence of Synechococcus CC9311: insights into adaptation to a coastal environment. *Proc. Natl. Acad. Sci.* **103,** 13555–13559 (2006).
6. Sunda, W. G., Swift, D. G. & Huntsman, S. A. Low iron requirement for growth in oceanic phytoplankton. *Nature* **351,** 55–57 (1991).
7. Peers, G. & Price, N. M. Copper-containing plastocyanin used for electron transport by an oceanic diatom. *Nature* **441,** 341–344 (2006).
8. Mahowald, N. M. *et al.* Atmospheric global dust cycle and iron inputs to the ocean. *Glob. Biogeochem. Cycles* **19,** GB4025 (2005).
9. Prospero, J. M. *et al.* in *Nitrogen Cycling in the North Atlantic Ocean and its Watersheds* (ed. Howarth, R. W.) 27–73 (Springer Netherlands, 1996). at <http://link.springer.com/chapter/10.1007/978-94-009-1776-7_2>
10. Biller, D. V. & Bruland, K. W. The central California Current transition zone: A broad region exhibiting evidence for iron limitation. *Prog. Oceanogr.* **120,** 370–382 (2014).

11. Mackey, K. R. M., Chien, C.-T. & Paytan, A. Microbial and biogeochemical responses to projected future nitrate enrichment in the California upwelling system. *Front. Microbiol.* **5,** (2014).
12. Hunter-Cevera, K. R. Population dynamics and diversity of Synechococcus on the New England Shelf. (Massachusetts Institute of Technology, 2014). at <http://dspace.mit.edu/handle/1721.1/92591>
13. Wu, J. & Luther, G. W. Spatial and temporal distribution of iron in the surface water of the northwestern Atlantic Ocean. *Geochim. Cosmochim. Acta* **60,** 2729–2741 (1996).
14. Webb, E. A., Moffett, J. W. & Waterbury, J. B. Iron Stress in Open-Ocean Cyanobacteria (Synechococcus, Trichodesmium, andCrocosphaera spp.): Identification of the IdiA Protein. *Appl. Environ. Microbiol.* **67,** 5444–5452 (2001).
15. Allen, A. E. *et al.* Whole-cell response of the pennate diatom Phaeodactylum tricornutum to iron starvation. *Proc. Natl. Acad. Sci.* **105,** 10438–10443 (2008).
16. La Roche, J., Boyd, P. W., McKay, R. M. L. & Geider, R. J. Flavodoxin as an in situ marker for iron stress in phytoplankton. *Nature* **382,** 802–805 (1996).
17. Escolar, L., Pérez-Martín, J. & Lorenzo, V. de. Opening the Iron Box: Transcriptional Metalloregulation by the Fur Protein. *J. Bacteriol.* **181,** 6223–6229 (1999).
18. Dautant, A. *et al.* Structure of a monoclinic crystal from of cyctochrome b1 (Bacterioferritin) from E. coli. *Acta Crystallogr. D Biol. Crystallogr.* **54,** 16–24 (1998).
19. Castruita, M. *et al.* Overexpression and Characterization of an Iron Storage and DNA-Binding Dps Protein from Trichodesmium erythraeum. *Appl. Environ. Microbiol.* **72,** 2918–2924 (2006).

20. Wu, J., Sunda, W., Boyle, E. A. & Karl, D. M. Phosphate Depletion in the Western North Atlantic Ocean. *Science* **289,** 759–762 (2000).
21. Coleman, M. L. & Chisholm, S. W. Ecosystem-specific selection pressures revealed through comparative population genomics. *Proc. Natl. Acad. Sci.* **107,** 18634–18639 (2010).
22. Gallien, S. *et al.* Targeted Proteomic Quantification on Quadrupole-Orbitrap Mass Spectrometer. *Mol. Cell. Proteomics* **11,** 1709–1723 (2012).
23. Fitzgerald, M. P., Rogers, L. J., Rao, K. K. & Hall, D. O. Efficiency of ferredoxins and flavodoxins as mediators in systems for hydrogen evolution. *Biochem. J.* **192,** 665–672 (1980).
24. Bertrand, E. M. *et al.* Methionine synthase interreplacement in diatom cultures and communities: Implications for the persistence of B12 use by eukaryotic phytoplankton. *Limnol. Oceanogr.* **58,** 1431–1450 (2013).
25. Bergquist, B. A. & Boyle, E. A. Dissolved iron in the tropical and subtropical Atlantic Ocean. *Glob. Biogeochem. Cycles* **20,** GB1015 (2006).
26. Martiny, A. C. *et al.* Strong latitudinal patterns in the elemental ratios of marine plankton and organic matter. *Nat. Geosci.* **6,** 279–283 (2013).
27. Bertilsson, S., Berglund, O., Karl, D. M. & Chisholm, S. W. Elemental composition of marine Prochlorococcus and Synechococcus: Implications for the ecological stoichiometry of the sea. *Limnol. Oceanogr.* **48,** 1721–1731 (2003).
28. Rusch, D. B., Martiny, A. C., Dupont, C. L., Halpern, A. L. & Venter, J. C. Characterization of Prochlorococcus clades from iron-depleted oceanic regions. *Proc. Natl. Acad. Sci.* **107,** 16184–16189 (2010).

29. Ahlgren, N. A. *et al.* The unique trace metal and mixed layer conditions of the Costa Rica upwelling dome support a distinct and dense community of Synechococcus. *Limnol. Oceanogr.* **59,** 2166–2184 (2014).
30. Sedwick, P. N. *et al.* Iron in the Sargasso Sea (Bermuda Atlantic Time-series Study region) during summer: Eolian imprint, spatiotemporal variability, and ecological implications. *Glob. Biogeochem. Cycles* **19,** n/a–n/a (2005).
31. Saito, M. A. *et al.* Multiple nutrient stresses at intersecting Pacific Ocean biomes detected by protein biomarkers. *Science* **345,** 1173–1177 (2014).
32. Casey, J. R., Lomas, M. W., Mandecki, J. & Walker, D. E. Prochlorococcus contributes to new production in the Sargasso Sea deep chlorophyll maximum. *Geophys. Res. Lett.* **34,** L10604 (2007).
33. Noble, A. E. *et al.* Basin-scale inputs of cobalt, iron, and manganese from the Benguela-Angola front to the South Atlantic Ocean. *Limnol. Oceanogr.* **57,** 989–1010 (2012).
34. Field, M. P., Cullen, J. T. & Sherrell, R. M. Direct determination of 10 trace metals in 50 mL samples of coastal seawater using desolvating micronebulization sector field ICP-MS. *J Anal Spectrom* **14,** 1425–1431 (1999).
35. Sunda, W. & Huntsman, S. Effect of pH, light, and temperature on Fe–EDTA chelation and Fe hydrolysis in seawater. *Mar. Chem.* **84,** 35–47 (2003).
36. Lis, H., Kranzler, C., Keren, N. & Shaked, Y. A Comparative Study of Iron Uptake Rates and Mechanisms amongst Marine and Fresh Water Cyanobacteria: Prevalence of Reductive Iron Uptake. *Life* **5,** 841–860 (2015).

37. Keller, A., Nesvizhskii, A. I., Kolker, E. & Aebersold, R. Empirical Statistical Model To Estimate the Accuracy of Peptide Identifications Made by MS/MS and Database Search. *Anal. Chem.* **74,** 5383–5392 (2002).
38. De Hoon, M. J. L., Imoto, S., Nolan, J. & Miyano, S. Open source clustering software. *Bioinformatics* **20,** 1453–1454 (2004).
39. Saito, M. A. *et al.* Iron conservation by reduction of metalloenzyme inventories in the marine diazotroph Crocosphaera watsonii. *Proc. Natl. Acad. Sci.* **108,** 2184–2189 (2011).
40. Lange, V. *et al.* Targeted Quantitative Analysis of Streptococcus pyogenes Virulence Factors by Multiple Reaction Monitoring. *Mol. Cell. Proteomics* **7,** 1489–1500 (2008).
41. Cutter, G. A. & Bruland, K. W. Rapid and noncontaminating sampling system for trace elements in global ocean surveys. *Limnol. Oceanogr. Methods* **10,** 425–436 (2012).
42. Conway, T. M., Rosenberg, A. D., Adkins, J. F. & John, S. G. A new method for precise determination of iron, zinc and cadmium stable isotope ratios in seawater by double-spike mass spectrometry. *Anal. Chim. Acta* **793,** 44–52 (2013).
43. Conway, T. M. & John, S. G. Quantification of dissolved iron sources to the North Atlantic Ocean. *Nature* **511,** 212–215 (2014).
44. Zimmer, L. A. & Cutter, G. A. High resolution determination of nanomolar concentrations of dissolved reactive phosphate in ocean surface waters using long path liquid waveguide capillary cells (LWCC) and spectrometric detection. *Limnol. Oceanogr. Methods* **10,** 568–580 (2012).
45. Zhang, J.-Z. Shipboard automated determination of trace concentrations of nitrite and nitrate in oligotrophic water by gas-segmented continuous flow analysis with a liquid waveguide capillary flow cell. *Deep Sea Res. Part Oceanogr. Res. Pap.* **47,** 1157–1171 (2000).

Figure Legends

Figure 1: (A) Map of the US North Atlantic Zonal GEOTRACES sampling stations and locations where *Synechococcus* WH8102 and WH8020 were isolated, and the location of BATS. (B) Concentrations of nitrate, phosphate, and dissolved Fe along the transect from 28-51m depth. (C) Ratios of dissolved Fe : nitrate (pM:nM) and nitrate : phosphate (nM:nM) along the transect.

Figure 2: Physiological and photosynthetic responses of oceanic WH8102 (left, A-E) and coastal WH8020 (right, F-J) to [Fe']. Vertical dashed lines in (A,F) and bars in (B,G) indicate the concentration of Fe' (plotted as log[Fe']) at which a given physiological parameter showed a threshold response (see Methods). Growth rate (circles) and photosynthetic efficiency (F_v/F_M measured at the time the protein samples were collected, shaded regions) are shown in (A,F). ETC = membrane proteins in the photosynthetic electron transport chain. Growth curves are shown in (C,H) and photosynthetic efficiency (Fv/F_M) values collected each day are shown in (D,I). Legend for (C,D,H,I) is shown below panel (I). (E,J) Heatmap of photosynthetic electron transport chain proteins for *Synechococcus sp*. strains WH8102 (E) and WH8020 (J). Normalized spectral counts are given in SI Appendix Table S4. Color indicates higher (yellow) or lower (purple) abundance relative to the centered mean value (black).

Figure 3: (A) Abundance of Fe related proteins in coastal *Synechococcus sp*. strain WH8020 in response to [Fe'] (gene IDs correspond to genes in SI Appendix Table S1). (B) Venn diagram of Fe response genes (SI Appendix Table S1) in the genomes of oceanic strain WH8102, and coastal strains WH8020 and CC9311. (C) N costs associated with Fe response proteins in coastal *Synechococcus* WH8020 under high (>1 nM) and low (≤1 nM) Fe conditions (the expression

474 threshold for these proteins). Ferredoxin (2042) was ~100-fold less abundant than flavodoxin.
475 Although ferredoxin is more abundant under high Fe (see (A)), the effect is masked in (C) due to
476 the scale used for flavodoxin.

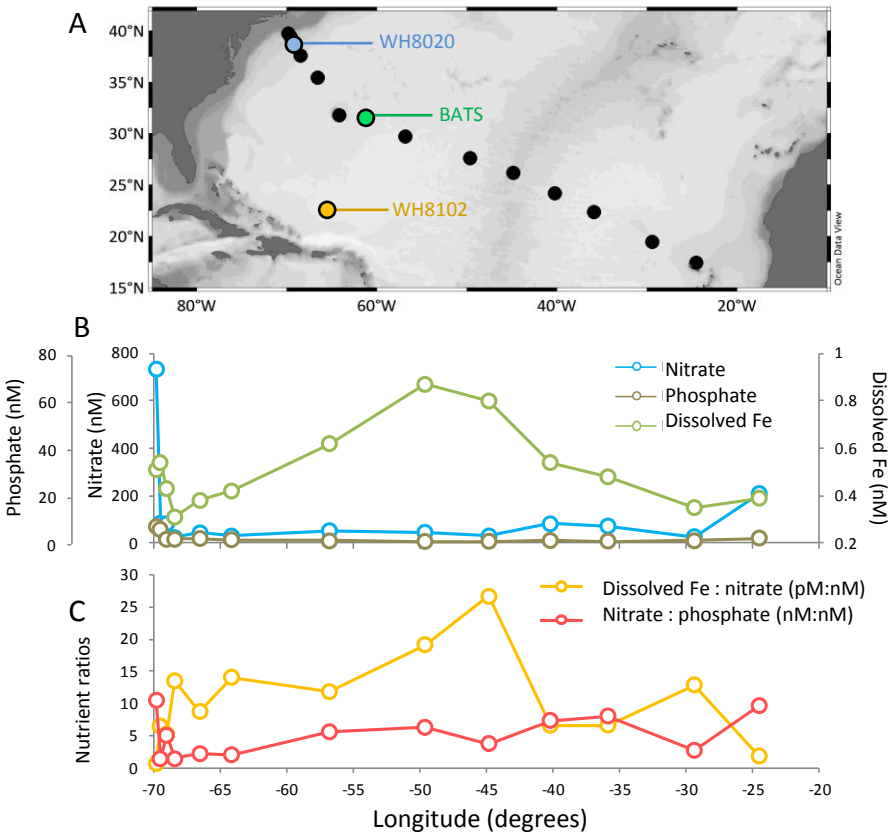
A
40°N
35°N
30°N
25°N
20°N
15°N
80°W
60°W
40°W
20°W
WH8020
BATS
WH8102
Ocean Data View
B
Phosphate (nM)
Nitrate (nM)
Dissolved Fe (nM)
Nitrate
Phosphate
Dissolved Fe
C
Nutrient ratios
Dissolved Fe : nitrate (pM:nM)
Nitrate : phosphate (nM:nM)
Longitude (degrees)

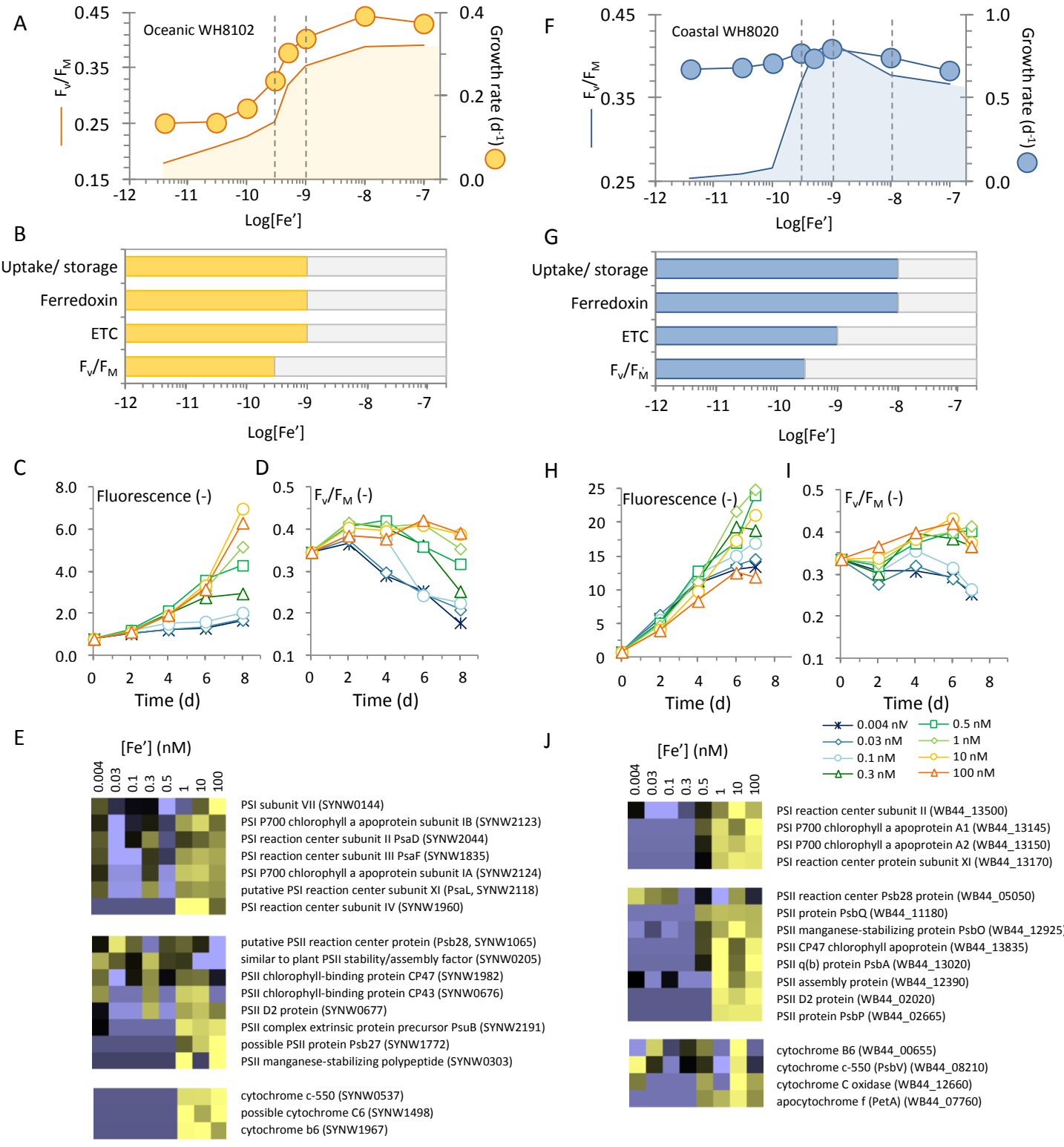
A
Oceanic WH8102
F_v/F_M
Growth rate (d^{-1})
Log[Fe']
F
Coastal WH8020
B
Uptake/ storage
Ferredoxin
ETC
F_v/F_M
G
C
Fluorescence (-)
Time (d)
D
F_v/F_M (-)
H
I
0.004 nM
0.03 nM
0.1 nM
0.3 nM
0.5 nM
1 nM
10 nM
100 nM
E
[Fe'] (nM)
0.004
0.03
0.1
0.3
0.5
1
10
100
PSI subunit VII (SYNW0144)
PSI P700 chlorophyll a apoprotein subunit IB (SYNW2123)
PSI reaction center subunit II PsaD (SYNW2044)
PSI reaction center subunit III PsaF (SYNW1835)
PSI P700 chlorophyll a apoprotein subunit IA (SYNW2124)
putative PSI reaction center subunit XI (PsaL, SYNW2118)
PSI reaction center subunit IV (SYNW1960)
putative PSII reaction center protein (Psb28, SYNW1065)
similar to plant PSII stability/assembly factor (SYNW0205)
PSII chlorophyll-binding protein CP47 (SYNW1982)
PSII chlorophyll-binding protein CP43 (SYNW0676)
PSII D2 protein (SYNW0677)
PSII complex extrinsic protein precursor PsuB (SYNW2191)
possible PSII protein Psb27 (SYNW1772)
PSII manganese-stabilizing polypeptide (SYNW0303)
cytochrome c-550 (SYNW0537)
possible cytochrome C6 (SYNW1498)
cytochrome b6 (SYNW1967)
J
[Fe'] (nM)
PSI reaction center subunit II (WB44_13500)
PSI P700 chlorophyll a apoprotein A1 (WB44_13145)
PSI P700 chlorophyll a apoprotein A2 (WB44_13150)
PSI reaction center protein subunit XI (WB44_13170)
PSII reaction center Psb28 protein (WB44_05050)
PSII protein PsbQ (WB44_11180)
PSII manganese-stabilizing protein PsbO (WB44_12925)
PSII CP47 chlorophyll apoprotein (WB44_13835)
PSII q(b) protein PsbA (WB44_13020)
PSII assembly protein (WB44_12390)
PSII D2 protein (WB44_02020)
PSII protein PsbP (WB44_02665)
cytochrome B6 (WB44_00655)
cytochrome c-550 (PsbV) (WB44_08210)
cytochrome C oxidase (WB44_12660)
apocytochrome f (PetA) (WB44_07760)

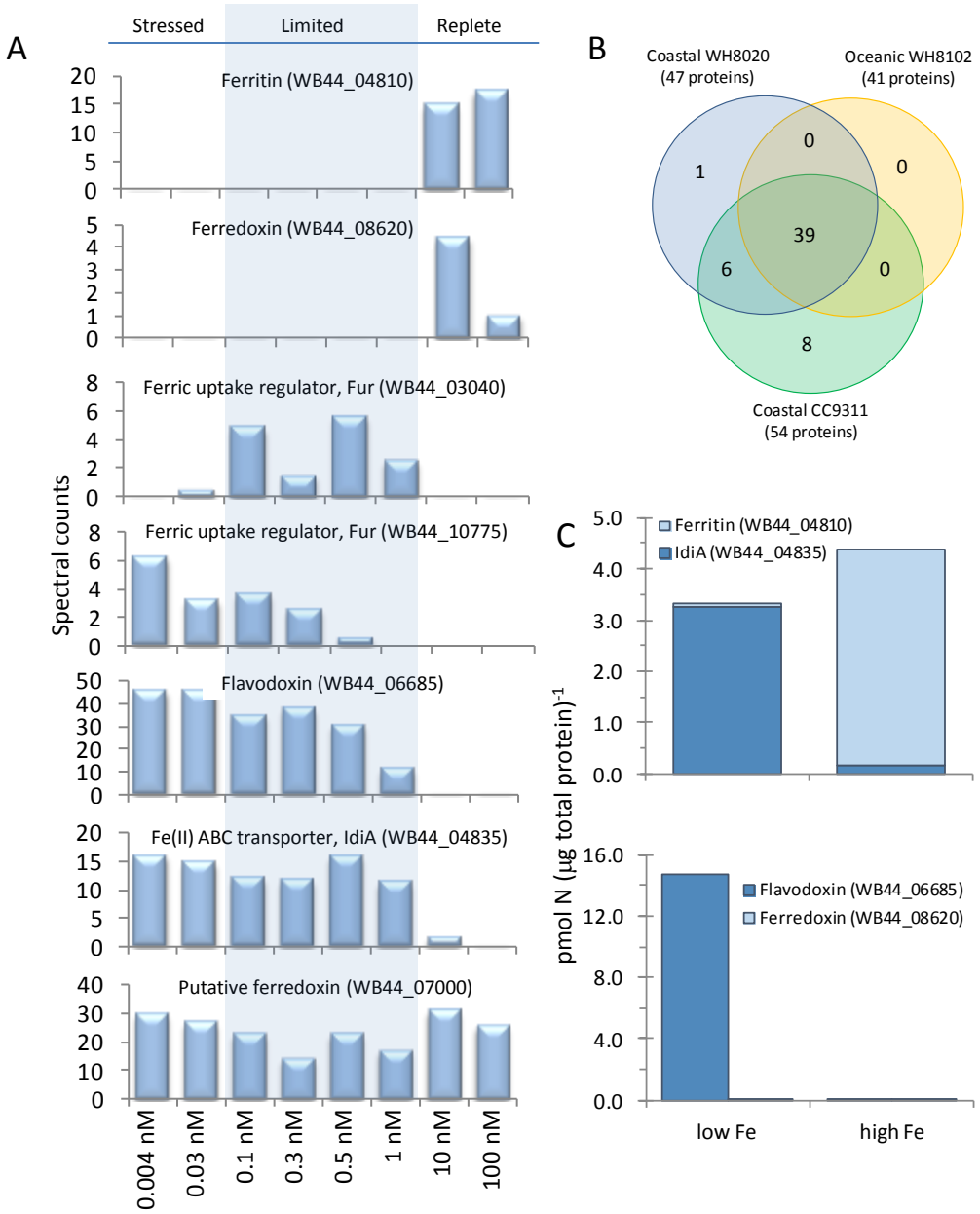
A
Stressed
Limited
Replete
Ferritin (WB44_04810)
Ferredoxin (WB44_08620)
Ferric uptake regulator, Fur (WB44_03040)
Ferric uptake regulator, Fur (WB44_10775)
Flavodoxin (WB44_06685)
Fe(II) ABC transporter, IdiA (WB44_04835)
Putative ferredoxin (WB44_07000)
Spectral counts
0.004 nM
0.03 nM
0.1 nM
0.3 nM
0.5 nM
1 nM
10 nM
100 nM
B
Coastal WH8020
(47 proteins)
Oceanic WH8102
(41 proteins)
Coastal CC9311
(54 proteins)
1
0
0
39
6
0
8
C
Ferritin (WB44_04810)
IdiA (WB44_04835)
Flavodoxin (WB44_06685)
Ferredoxin (WB44_08620)
pmol N (µg total protein)-1
low Fe
high Fe